

The Lunar Opposition Surge:
Observations by **Clementine**

Bonnie J. Buratti, John Hillier, and Michael Wang

Jet Propulsion Laboratory

California Institute of Technology

4800 Oak Grove Dr. 183-501

Pasadena, CA 91109

Correspondence address:

Bonnie J. Buratti

JPL 183-501

4800 Oak Grove Dr.

Pasadena, CA 91109

(818) 354-7427

FAX (818) 354-0966

buratti@jplpds.jpl.nasa.gov

19 pages

7 figures

ABSTRACT

The Clementine mission to the Moon in 1994 provided the first multispectral observations of the lunar opposition surge below a few degrees. The brightness of the Moon increases more than 40% between solar phase angles of 4° and 0° . The opposition effect exhibits a small wavelength dependence: the surge is 3-4% larger at $0.41 \mu\text{m}$ than at $1.00 \mu\text{m}$. This result suggests that the principal cause of the lunar opposition surge is shadow-hiding rather than coherent backscatter. The amplitude of the effect depends significantly on terrain: the surge is about 10% greater in the lunar highlands. We attribute this difference to textural variations between the two terrains. The Clementine measurements provide a new basis for deriving spectral geometric albedos, phase integrals, and Bond albedos. We find a value of 0.11 ± 0.01 for the lunar bolometric Bond albedo. This value is at the low end of the historical published values, but not as low as the recent result of 0.080 ± 0.002 derived by Helfenstein et al. (Icarus, 1996, in press)

II. INTRODUCTION

The Moon exhibits a non-linear surge in brightness as its face becomes fully illuminated to an observer. The canonical explanation for this "opposition surge" is a shadow-hiding mechanism, in which mutual shadows cast by particles in the upper regolith are hidden at opposition but become rapidly visible as the phase angle increases (Irvine, 1966; Hapke, 1986). Because the character of the opposition effect is a sensitive indication of the surficial compaction state and particle size (Hapke, 1986) - and thus of lunar geophysical processes - observations at small solar phase angles are important to obtain. Recent observations have shown that many solar system bodies exhibit, in addition to an opposition effect that is typically seen at solar phase angles less than 6° , extremely narrow and large surges in brightness below one degree (Buratti et al., 1992; Thompson and Lockwood, 1992). Standard shadow hiding models require extremely (and probably unreasonably) porous surfaces to explain these narrow opposition surges (see Domingue and Hapke, 1991). Problems of this sort have led to the suggestion that a second mechanism, coherent backscatter, may be responsible for the observed surge (Hapke, 1990; Mishchenko, 1992). In this mechanism, photons following identical but reversed paths in a surface interfere constructively in exactly the backscattering direction leading to up to a factor of two increase in brightness. A narrowly peaked opposition surge was observed on lunar samples measured in the lab, although these measurements did not extend to phase angles less than one degree (Hapke et al., 1993).

The Moon's finite angular size as seen from Earth precludes groundbased observations of its solar phase curve below ~ 0.5 degree: at this point a lunar eclipse occurs. Previous Apollo photographic observations of the Moon suggested that the Moon has a huge opposition spike below 0.75° (Pohn et al., 1969; Wildey, 1978). The Clementine mission enabled the first electronic, multispectral observations of the Moon at very small solar phase angles. Several hundred images of the opposition surge of the Moon under one degree were obtained by the spacecraft. This data set is by far the most extensive for any celestial object at small solar phase angles, and they offer an unprecedented opportunity to study the opposition effect on a planetary surface. The data are of course disk resolved, and extend over the wavelength range of $0.41 \mu\text{m}$ to $1.0 \mu\text{m}$ for the UV/Visible camera and $1.0 \mu\text{m}$ to $2.8 \mu\text{m}$ for the Near IR camera. Another important feature of the Clementine observations is that a change of

several degrees in solar phase angle appears on one image; it is thus possible to create a highly accurate phase curve in those last few degrees. The typical scatter that appears in published phase curves at small phase angles is about 0.5 astronomical magnitudes (Helfenstein et al. , 1996); the Clementine data exhibits scatter of $\pm 1-5\%$ (the variations are primarily due to albedo changes rather than error) . The multispectral observations offer a critical test of the mechanism responsible for the lunar opposition surge: the shadowing mechanism should be more pronounced at wavelengths for which the albedo is lower (since shadows are not partly illuminated), while coherent backscatter should show the opposite relationship, because it is a multiple scattering phenomenon.

For a description of the Clementine spacecraft and its instruments, and an overview of the scientific results , see Nozette et al. (1994).

III. OBSERVATIONS AND DATA ANALYSIS

The Clementine images at small solar phase angles were obtained near the middle of the mission and near the lunar equator. We have chosen to analyze the data from the UV/Vis camera for the following reasons: the calibration factors are better understood than those for the NIR, the HiRes or LWIR cameras; it is easier to compare our results with ground-based observations of the Moon and other bodies; and the complicating factor of thermal emission is minimized. The UV/Vis is also best suited for studying the effect of albedo on the opposition surge , because the albedo of the Moon changes most significantly between 0.4 and $0.8 \mu\text{m}$. Table 1 summarizes the images used in our study.

In each of the images obtained at small solar phase angles, a small (0.50 degree wide) bright spot appears at the point of zero degrees. This spot is not instrumental , and it is also seen on NIR images (a search of HiRes images has not yet been made). Figure 1 shows typical images (orbits 149 and 167) while Figure 2 presents a scan extracted from zero degrees to the edge of one of the images. For comparison, we show solar phase curves for other bodies that exhibit opposition surges at small solar phase angles. The surge seen by Clementine is qualitatively similar to that reported by Pohn et al. (1969) and Wildey (1978) on Apollo photographs, although our measurements show that the effect is somewhat greater than that derived from the photographs ($43\% \pm 2\%$ in the visual region of the spectrum between 4° and 0° , as opposed to 37% reported by Pohn et al. (1969))

Two important factors to investigate for the lunar opposition surge are the dependence of the effect on 1) wavelength, and 2) terrain type. Wavelength dependence is a clear indication of the mechanism responsible for the effect, while terrain dependence indicates differences in surface textural properties between the lunar highlands and maria. Scans of the opposition surge in the five primary filters of the UV/Vis were extracted from images in orbits 150, 151, 154, 155, 165, 166, 167, 168, and 169. The data from these images were extracted with the following procedure. First, the scattering angles (incidence, emission, and solar phase angles) at the center of each 2 X 2 block of pixels were calculated with procedures provided by the JPL Navigation Section's SPICE library. The reflectance from each group of 4 pixels was then averaged (the averaging procedure was required to save disk space). The data for each image were then binned in 0.02° increments of phase angle, and the resulting averaged data were normalized such that the average reflectance in the lowest bin (0 - 0.02°) is 1.0. The data for images in each filter were then added together. The resulting averaged lunar opposition surges at 0.41 μm, 0.75 μm, and 1.0 μm, representing the full range in wavelength for the UV/Vis camera, are shown in Figure 3.

To quantify the dependence of the surge on wavelength, a line was fit to the phase curves between 0° and 4° (Brightness = $A - t B\lambda$; see Table 2). The formal values show that the amplitude of the surge is inversely correlated with wavelength, although by a small amount. At a phase angle of 4°, this effect is most clearly seen: the reflectance is 0.690 for the A filter (0.41 μm), 0.703 for filter B (0.75 μm), 0.715 for filter C (0.90 μm), 0.720 for filter D (0.95 μm), and 0.715 for filter E (1.00 μm) (Table 3). This effect of "phase reddening" has been described previously for the Moon and other bodies (e.g., Lane and Irvine, 1973) at larger phase angles. Because of the increase in the Moon's albedo with wavelength from visible to near-IR wavelengths, the shadow-hiding mechanism predicts that the opposition surge is inversely correlated with wavelength to produce a reddening of the lunar albedo as the phase angle increases (Irvine, 1966, Helfenstein et al., 1996). Early measurements (Mikhail, 1970) confirm the prediction. The observations by Gehrels et al. (1964) over 11 lunar regions at the very smallest phase angles (2° - 0.8° degrees) show no clear trend. Goniometric measurements on an Apollo 11 sample from Tranquility base show an inverse phase reddening (O'Leary and Briggs, 1970) under 5°. In the most comprehensive prior study of the wavelength dependence of the opposition surge,

Helpfenstein et al. (1996) conclude that the strength of the surge decreases with increasing albedo. However, their color data include no observations below 5° . Our measurements are the first to suggest phase reddening of the opposition surge for the Moon as a whole for small phase angles (< 50).

A correlation between lunar terrain type and the character of the opposition surge was reported by Wildey and Pohn (1969), who show that the surge near the Tranquility base is only 7% between phase angles of 1.5° and 0° , while the surge for the Moon as a whole from Apollo photogrammetry is 19% over the same range, Gehrels et al. (1964) measured opposition surges on 13 separate regions (the minimum phase angle ranged from 0.8 to 1.0 degree). Although the amplitude and width of the effect varies from region to region, no clear trend with terrain type, albedo, etc. is evident. To derive a possible correlation between the lunar opposition surge and the two major terrain types (highlands and maria), we constructed composite curves representing these areas. Images obtained at zero degrees phase angle in orbit 167 are located in the highland regions near 5 degree-s E. longitude, while orbit 152 contains images of the opposition surge in Mare Tranquilitatis (both regions are near the equator, where all the opposition images are located). Figure 4 shows the two composite curves and a ratio of the highland to maria regions (because most images have a mixture of the two terrain types, we were able to construct well-averaged curves for $\alpha \leq 1.2^\circ$ only). Clearly, there is a trend, with the amplitude of the surge about 10% greater for the highlands. This trend is in the same direction as that reported by Wildey and Pohn (1969), although our measurements do not show as significant an effect; our data reveal a surge of 16% between 1.2° and 0° for Mare Tranquilitatis, compared with Wildey and Pohn's (1969) measurement of only 7% between 0° and 1.5° .

The Clementine spacecraft's observations of the lunar opposition effect enable an accurate measurement of the Moon's geometric albedo (p), phase integral (q), and Bond albedo (A_B). By definition, the geometric albedo can only be known from observations at opposition. In their extensive study of the integral geometric albedo of the Moon, Lane and Irvine (1973) point out that the values they derived based on a linear extrapolation of the lunar phase curve were underestimated by a factor of 44% to 100%. Similarly, Helpfenstein et al. (1996) obtain an estimate of the normal reflectance (which is very nearly equal to the geometric albedo in the case of the Moon) that is 50% uncertain (Figure 1c).

Their values for p and q (Figure 7) are based on a fit to a Hapke-type model.

A composite lunar phase curve for three colors is illustrated in Figure 5; the data between 0° and 4° are from the Clementine UV/Vis camera while the remaining data are from Lane and Irvine (1973); the data for each color are normalized at 4° . Table 4 lists the corresponding geometric albedos in the Clementine filters; these geometric albedos are based on those obtained by Lane and Irvine (1973), but with Clementine's measured opposition surge. When the Clementine cameras are fully calibrated, the value of the normal reflectance at zero degrees will yield a direct measurement of the geometric albedo. Although there were no Clementine filters corresponding to the astronomical visual filter ($0.55 \mu\text{m}$) the interpolated value for the visual geometric albedo is 0.16 ± 0.01 . This value is higher than those of 0.14-0.15 obtained previously (Helfenstein and Veverka, 1987; Lumme and Irvine, 1982).

The phase integral (Russell, 1916) was computed with a 2-point Gaussian quadrature (Chandrasekhar, 1960) for the three phase curves in Figure 5. The resulting values, along with the Bond albedo ($A_B = p*q$), are listed in Table 4 with previous values for comparison. At the visual wavelengths, the increase in geometric albedo is offset by a decrease in the phase integral, so that the new values of the Bond albedo are not very different from Lane and Irvine (1973), although our values are higher than those of Helfenstein et al. (1996). In the near-IR ($1.0 \mu\text{m}$) our value for the lunar Bond albedo is significantly higher than previous estimates.

The bolometric (or radiometric) Bond albedo, an important quantity for understanding the thermal properties of the Moon, is given by:

$$A_B = \int_0^\infty F_o(\lambda) p_\lambda q_\lambda d\lambda / \int_0^\infty F_o(\lambda) d\lambda \quad (1)$$

where $F_o(\lambda)$ is the flux of the sun at wavelength λ . The values of q were interpolated for the C and D filters (see Table 3). For p and q between 1.0 and $2.5 \mu\text{m}$, we extrapolated from our values with a wavelength dependency derived from Helfenstein et al. (1996). Using the values for the flux of the sun listed in Allen (1976), we find a bolometric Bond albedo of 0.11 ± 0.01 , based on data

between 0.41 μm and 2.5 μm . This value is at the low range of previously published values of 0.11-0.136 (Lane and Irvine, 1973 and references cited therein; Helfenstein and Veverka, 1987), but not as low as the value of 0.080 \pm 0,002 recently derived by Helfenstein et al. (1996). Our value is lower than most previous values because we have fully included the opposition surge, but it is still higher than Helfenstein et al.'s value because of our different spectral dependencies for p and q (see Table 3) in the visible.

III. MODELING

The color-dependent opposition curves provided by Clementine render the first opportunity to critically test which mechanism is responsible for the opposition surge. According to the shadow-hiding model, the width of the opposition surge depends primarily on the porosity of the surface and therefore should be relatively independent of wavelength (in the case of bodies for which multiple scattering is important, and which have increasing albedos with wavelength, the surge should become less significant with increasing wavelength). In contrast, the coherent backscatter model predicts a strong wavelength dependence to the opposition surge. These differences provide a diagnostic we can use to help distinguish which mechanism is most responsible for the observed surge. Our result that there is only a small color dependence to the lunar opposition surge (Figure 3) suggests that coherent backscatter is not the dominant mechanism for the Moon's surge in brightness. Moreover, the dependence is in the wrong direction. Mishchenko (1992) suggests that the wavelength dependence of coherent backscatter might disappear if there is a wide distribution of particle sizes, *but only for icy surfaces*. For silicate surfaces, the effect remains "substantially wavelength-dependent".

On the other hand, a standard shadow-hiding model yields unreasonably high values for the lunar porosity. Porosity values requiring '90% void space are needed to fit the observations with such models (Seeliger, 1887; Irvine, 1966, Hapke, 1986). Recently, however, we have developed a modified shadow hiding model (Hillier, 1996) that suggests shadow hiding may not require extremely porous surfaces. The model is based on Hapke's (1986) shadow hiding model but allows for 2-layer surfaces in which the particle properties (for example the particle size) can vary between the layers. Figure 6 shows that the modified model can provide a good fit to the lunar opposition surge data while requiring

a less porous (67% or perhaps even less) surface than the standard shadow hiding model if the particle size decreases towards the surface. Apollo core samples show the lunar surface to be relatively well mixed with grain size relatively independent of depth (though with a slight suggestion of decreasing particle size towards the surface; McKay et al., 1977, 1991). However, the upper millimeter or so (a significant fraction of the optically active surface) of the regolith is expected to undergo intense micrometeoritic bombardment (Gault et al., 1974). While it is not entirely clear whether such bombardment would lead to smaller particles, soil maturation models do suggest a decrease in particle size with maturity (McKay et al., 1991) and thus a lower particle size in the very upper layers may not be unreasonable. The modified shadow hiding model therefore appears promising as an explanation for the observed opposition surges.

Another possibility is that individual particles simply have sharply peaked single particle phase functions. Our own measurements of glass spheres at small phase angles (down to 0.1°) show that they have large surges in brightness (up to 40%) in the last few degrees (Figure 7). Since the lunar fines contain agglutinated spheres (McKay et al., 1991), an intrinsic sharply peaked phase function is a reasonable possibility.

IV. CONCLUSIONS AND DISCUSSION

The Clementine spacecraft provided the first multispectral observations of the lunar opposition effect. Between 4° and 0° the brightness of the Moon increases by about 40-45%. The amplitude of the surge depends weakly on wavelength; the blue region of spectrum exhibits a '3-4% larger effect. There is a significant dependence of the opposition surge on lunar terrain type. On average, the opposition surge in the lunar maria is about 10% less than that seen in the highlands. If this difference is attributed to textural properties, it means the highlands are more tenuous than the maria. The textural difference could be attributed to the longer period of micrometeoritic bombardment to which the highlands have been subjected,

If coherent backscatter is important on the Moon, the opposition surge would be more pronounced in the Clementine E filter ($1.0 \mu\text{m}$), where the degree of multiple scattering should be the highest. This is definitely not the case. We conclude on the basis of this observation that shadow hiding is the primary

mechanism for the surge. A new two-layer model of shadow hiding (Hillier, 1996) yields reasonable values for the lunar porosity (-70%), The fact that there is only a small spectral dependence to the opposition surge means that multiple scattering is not important on the Moon. If it were, and shadow hiding were the principal mechanism, the red wavelengths should exhibit significantly smaller surges, because the shadows would be partly illuminated by multiply scattered photons. At every wavelength, only primary shadows are created.

Laboratory experiments on the photometric effects of multiple scattering do indeed show that a photometric model involving only singly scattered radiation applies to surfaces with normal reflectance less than 0.30 (Veverka et al., 1978). For the Saturnian satellites, multiple scattering is not important unless the normal reflectance is greater than 0.60 (Buratti, 1984). The fact that multiple scattering is unimportant on the Moon has been known for over 100 years: the solution to the equation of radiative transfer for single scattering from a surface is the well-known Lommel-Seeliger photometric function of the Moon. Similarly, near opposition the Moon is known to exhibit no limb darkening, the signature of multiple scattering (Schoenberg, 19'25; Minnaert, 1961), It is thus not surprising that coherent backscatter, a phenomenon that depends on multiple scattering, is not the principal mechanism for the lunar opposition surge,

Although our results suggest that shadow hiding (or possibly an intrinsically peaked single scattering phase function) is primarily responsible for the opposition surge seen on the Moon, it would be premature to say the effect of coherent backscatter is entirely absent. Laboratory measurements of Apollo samples down to 1° show the polarization signature expected for coherent backscatter (Hapke et al., 1993). Similarly, there is still the possibility that the terrain difference exhibited is due to higher reflectance (and thus more multiple scattering) in the lunar highlands, rather than textural properties. The accepted explanation for phase reddening of the Moon is the increased importance of multiple scattering as the wavelength increases (shadows, which are more pronounced at larger phase angles, are thus redder). It is reasonable to believe that multiple scattering becomes important at larger phase angles: the singly scattered portion of the radiation returned from the Moon is strongly backscattering (Buratti, 1985; Helfenstein and Veverka, 1987), while one would expect multiply scattered photons to be isotropic, or at least more isotropic. As the phase angle increases, the fraction of the observed photons that are

multiply scattered increases

The Clementine measurements of the opposition effect provide the first accurate multispectral phase curve of the Moon at small phase angles. When combined with ground based observations at higher phase angles, more accurate values of fundamental photometric and radiometric properties can be derived. The surge means that the spectral geometric albedo of the Moon is higher than previously realized, while the wavelength-dependent phase integral is lower. Our bolometric Bond albedo of 0.11 ± 0.01 is at the low range of previous values, but not as low as the value of 0.080 ± 0.002 found by Helfenstein et al. (1996) .

ACKNOWLEDGEMENTS

This work was performed at the Jet Propulsion Laboratory, California Institute of Technology, under contract with the National Aeronautics and Space Administration.

REFERENCES

- Allen, C.W. 1976. *Astrophysical Quantities*. The Athlone Press, London.
- Buratti, B, J, 1984. Voyager disk resolved photometry of the Saturnian satellites. *Icarus* 59, 392-405
- Buratti, B. J. 1985. Application of a radiative transfer model to bright icy satellites. *Icarus* 61, 208-217.
- Buratti, B. J., J, Gibson, and J. Mosher 1992. CCD observations of the Uranian satellites. *Astron. J.* 104, 1618-1622.
- Buratti, B. J., W. Smythe, R. M. Nelson, and V. Gharakhani 1988. Spectrogoniometer for measuring planetary surface materials at small phase angles. *Appl. Optics* 27, 161-165.
- Chandrasekhar, S. 1960. *Radiative Transfer*, Dover, New York.
- Domingue, D. L., B. W. Hapke, G. W. Lockwood and D. T. Thompson 1991. Europa's phase curve: Implications for surface structure. *Icarus* 90, 30-42.
- Gault, D. E., F. Horz, D. E. Brownlee, and J. B. Hartung 1974. Mixing of the lunar regolith. *Proc. Lunar Sci. Conf.* 5, 2365-2386.
- Gehrels, T., T. Coffeen, and D. Owings 1964. Wavelength dependence of polarization. III. The lunar surface. *Astron. J.* 69, 8'26-852.

- Goguen, J. D. 1996. A quantitative test of the applicability of independent scattering to high albedo planetary regoliths. *Icarus*, in press.
- Hapke, B. 1966. An improved lunar theoretical photometric function. *Astron. J.* 71, 333-339.
- Hapke, B. 1986. Bidirectional reflectance spectroscopy. 4. The extinction coefficient and the opposition effect. *Icarus* 67, 264-280.
- Hapke, B. 1990. Coherent backscatter and the radar characteristics of outer planet satellites. *Icarus* 88, 407-417.
- Hapke, B., R. M. Nelson, and W. Smythe 1993. The opposition effect of the Moon: the contribution of coherent backscatter. *Science* 260, 509-511.
- Helfenstein, P., and J. Veverka 1987. photometric properties of lunar terrains derived from Hapke's equation. *Icarus* 72, 342-357.
- Helfenstein, P., J. Veverka, J. Hillier, C. M. Pieters, S. Pratt, J. W. Head, G. Neukum, H. Hoffmann, A. Oehler 1996. The wavelength dependence of lunar photometric properties. Submitted to *Icarus*.
- Hillier, J., P. Helfenstein., A. Verbiscer, J. Veverka, R. H. Brown, J. Goguen, and T. V. Johnson 1990. Voyager disk-integrated photometry of Triton. *Science* 250, 419-421.
- Hillier, J. 1996, in preparation.
- Irvine, W. M. 1966. The shadowing effect in diffuse radiation. *J. Geophys. Res.* 71, 2931-2937.
- Lane, A. and W. Irvine 1973. Monochromatic phase curves and albedos for the lunar disk. *Astron. J.* 78, 267-277.
- Lumme, K. and W. Irvine 1982. Radiative transfer in the surfaces of atmosphereless bodies. III. Interpretation of lunar photometry. *Astron. J.* 87 1076-1082.
- McKay, D. S., M.A.Dungan, R.V.Morris, and R.M. Fruland 1977. Grain size, petrology, and FMR studies of the double core 60009/10: a study of soil evolution. *Proc. Lunar Sci. Conf.* 8, 2929-2952.
- McKay, D. S., G. Heiken, A. Basu, G. Blanford, S. Simon, R. Reedy, B. M. French, and J. Papike 1991. The lunar regolith. in *The Lunar Sourcebook*, (Eds., G.H.Heiken, D.T. Vaniman, and B. M. French), Cambridge Univ. press, 285-356.
- Mikhail, J.S. 1970. Colour variations with phase of selected regions of the lunar surface. *Moon* 2, 167-201.
- Minnaert, M. 1961. Photometry of the Moon. In *The Solar System. III. Planets and Satellites*. (Eds., G.P. Kuiper and B. M. Middlehurst), Univ. of Chicago press,

Chicago.

- Mishchenko, M. I., 1992, The angular width of the coherent backscatter opposition effect: an application to icy outer planet satellites. *Astrophys. and Space Sci.* 194, 327-333.
- Nozette, S. and 33 coauthors 1994. The Clementine mission to the Moon: scientific overview. *Science* 206, 1835-1839.
- O'Leary, B. and F. Briggs 1970. Optical properties of Apollo 11 Moon samples. *J. Geophys. Res.* 75, 6532-6538.
- Pohn, H.A., H.W. Radin, and R.L. Wildey 1969. The Moon's photometric function near zero phase angle from Apollo 8 photography. *Astrophys. J.* 157, L193-L195.
- Russell, H.N. 1916, On the albedo of planets and their satellites. *Astrophys. J.* 43, 173-195.
- Schoenberg, E. 1925. Untersuchungen zur Theorie der Beleuchtung des Mondes auf Grund photometrischer Messungen. *Acta Soc. Sci. Fenn.* 9, 6-71.
- Seeliger, H. 1887. Zur theorie beleuchtung der grossen planeten insbesondere des Saturn, *Abhandl. Bayer. Akad. Wiss. Math. -Naturg.* Kl. II 16, 405-516
- Thompson, D. 'I'. , and G. W. Lockwood 1992. Photoelectric photometry of Europa and Callisto, 1976-1991. *J. Geophys. Res.* 97, 14,761-14,772.
- Veverka, J., J. Goguen, S. Yang, and J. Elliot 1978. Scattering of light from particulate surfaces I. A laboratory assessment of multiple scattering effects. *Icarus* 34, 406-414.
- Wildey, R. L. 1978. The Moon in heiligenschein. *Science* 200, 1265-1267.
- Wildey R. L. and H. A. Pohn 1969. The normal albedo of the Apollo 11 landing site and intrinsic dispersion in the lunar heiligenschein. *Astrophys. J.* 158, 1129-1130.

Table 1 - Summary of Clementine UV/Vis images at opposition used in this study

Orbit	# of images	filters
150	10	A, B, C, D, E
151	10	"
152	10	"
153	16	"
154	10	"
155	5	"
165	10	"
166	10	"
167	10	"
168	10	"
169	10	"

Table 2 - Fits of curves to $A + B\alpha$

Filter	λ_{eff}	Bandpass (FWHM)	A (± 0.01)	B (± 0.002)
A	0.41 μm	0.036 μm	1.00	-0.078
B	0.75 μm	0.0093 μm	1.00	-0.076
c	0.90 μm	0.0185 μm	1.00	-0.075
D	0.95 μm	0.0287 μm	1.00	-0.075
E	1.00 μm	0.0282 μm	0.99	-0.072

Table 3 - Wavelength dependent geometric albedos (p_λ), Bond albedos ($A_{B\lambda}$), and phase integrals (q_λ), with some previous values for comparison

Filter	$0^\circ/40$ (± 0.01)	p_λ^1 (± 0.005)	p_λ^2	p_λ^3	q_λ^1 (± 0.005)	q_λ^2	q_λ^3	$A_{B\lambda}^1$ (fool)	$A_{B\lambda}^2$	$A_{B\lambda}^3$
A	1.45	0.116	0.088	0.09	0.45	0.551	0.46	0.052	0.048	0.041
B	1.42	0.233	0.179	0.15	0.50	0.633	0.54	0.117	0.113	0.081
c	1.40	0.232	0.195	0.14	0.53		0.65	0.123		0.091
D	1.39	0.230	0.195	0.13	0.54		0.67	0.124		0.087
E	1.40	0.260	0.202	0.13	0.55	0.676	0.70	0.143	0.136	0.091

¹ This study; q_λ for filters C and D interpolated.

² Lane and Irvine (1973); correspondences made as follows: A \equiv 4155 Å; B \equiv 7297 Å; E \equiv 10635 Å; corresponding values for p_λ in filters C and D interpolated from their Figure 7.

³ Helfenstein et al. (1996); p_λ and q_λ from their Figure 7

FIGURE CAPTIONS

Figure 1. Images illustrating typical examples of opposition surges seen by the Clementine spacecraft: (a) Image LUC11225, in orbit 167, near 1° N latitude and 4° E longitude, in the lunar highlands at the east edge of Sinus Medii. (b) Images LUC30017 (top) and LUC30079 (bottom) in orbit 149, located in Mare Fecunditatis near latitudes and longitudes of (0°, 50° E) and (1° N, 51.5° E), respectively. In image LUC30017 the surge is the bright spot in the middle left side of the image (above the bright impact crater); in image LUC 30079 it is in the upper mid-left area of the picture.

Figure 2. A scan of the opposition surge extracted from the image in Figure 1 (a). For comparison, the opposition phase curves of Oberon and Europa are shown.

Figure 3. Averaged opposition phase curves of the Moon in 3 Clementine filters representing the wavelength range of the UV/Vis camera (for clarity the other two filters are not included).

Figure 4. Averaged opposition phase curves of the lunar maria (triangles) and highlands (filled squares). The ratio of highlands/maria (filled circles) shows that the highlands exhibit a surge about 10% higher than that of the maria in the last degree.

Figure 5. The integral phase curve of the Moon at three wavelengths. The small phase angles ($< 5^\circ$) were derived from Clementine data, while the larger phase angles were adopted and renormalized from Lane and Irvine (1973).

Figure 6, Fit of a two layer shadow hiding model to Clementine data at small solar phase angles. Shown are fits for various values of Hapke's (1986) opposition surge width parameter, h ,. The porosity, P , is related to h by $h = -3/8 \ln(P)$. The standard model requires low values of h (corresponding to $P \sim 90\%$) while the two-layer model allows higher values of h . We have accounted for the finite size of the sun as seen from the Moon in the model. In these models, the single scattering albedo (w) = 0.245 for both layers, and the ratio of the particle sizes in the two layers is (corresponding from lowest to highest value of h): 0.63, 0.29, 0.19, 0.14.

Figure 7. Laboratory measurements of the phase function of 400 μm glass beads. The experiment was done on a goniometer described in Buratti et al. (1988).



FIG 1 a

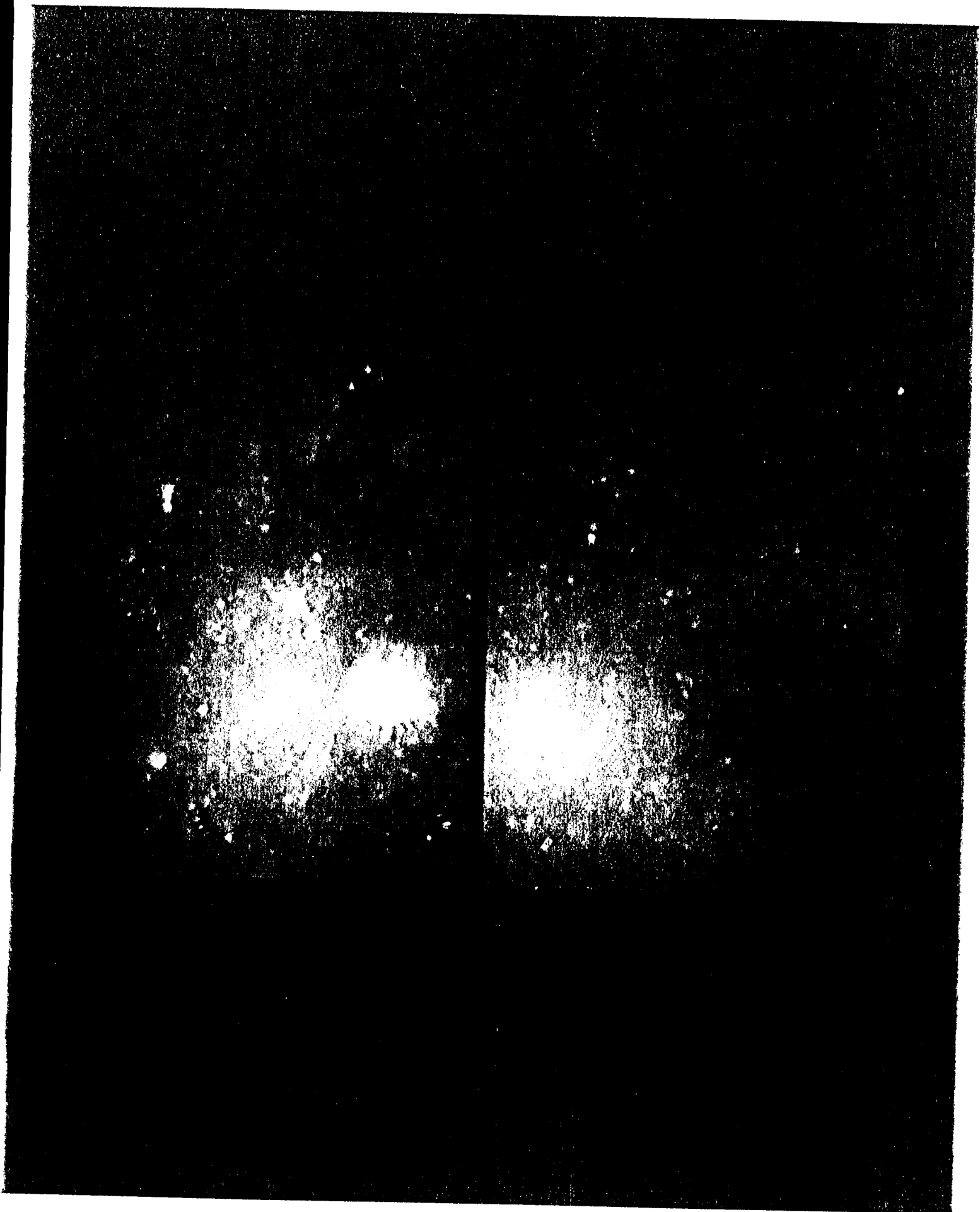


FIG 1b

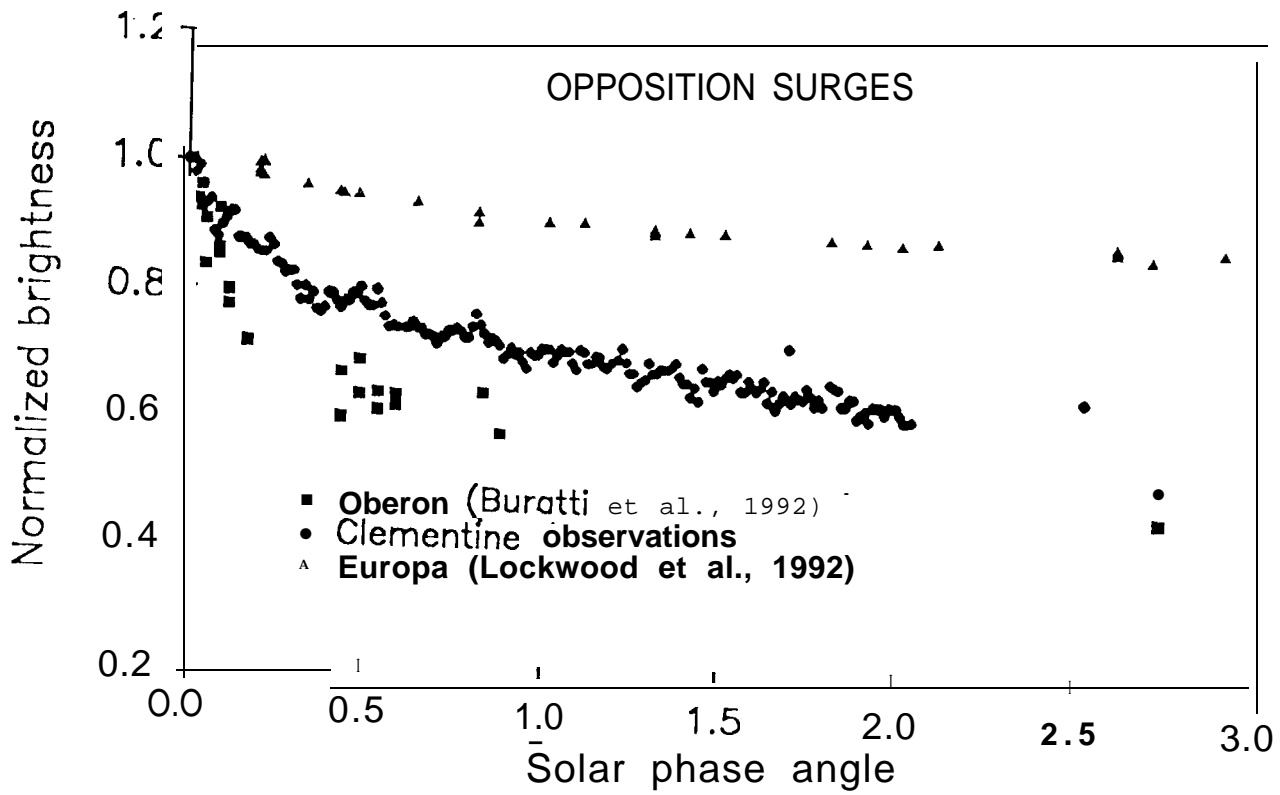
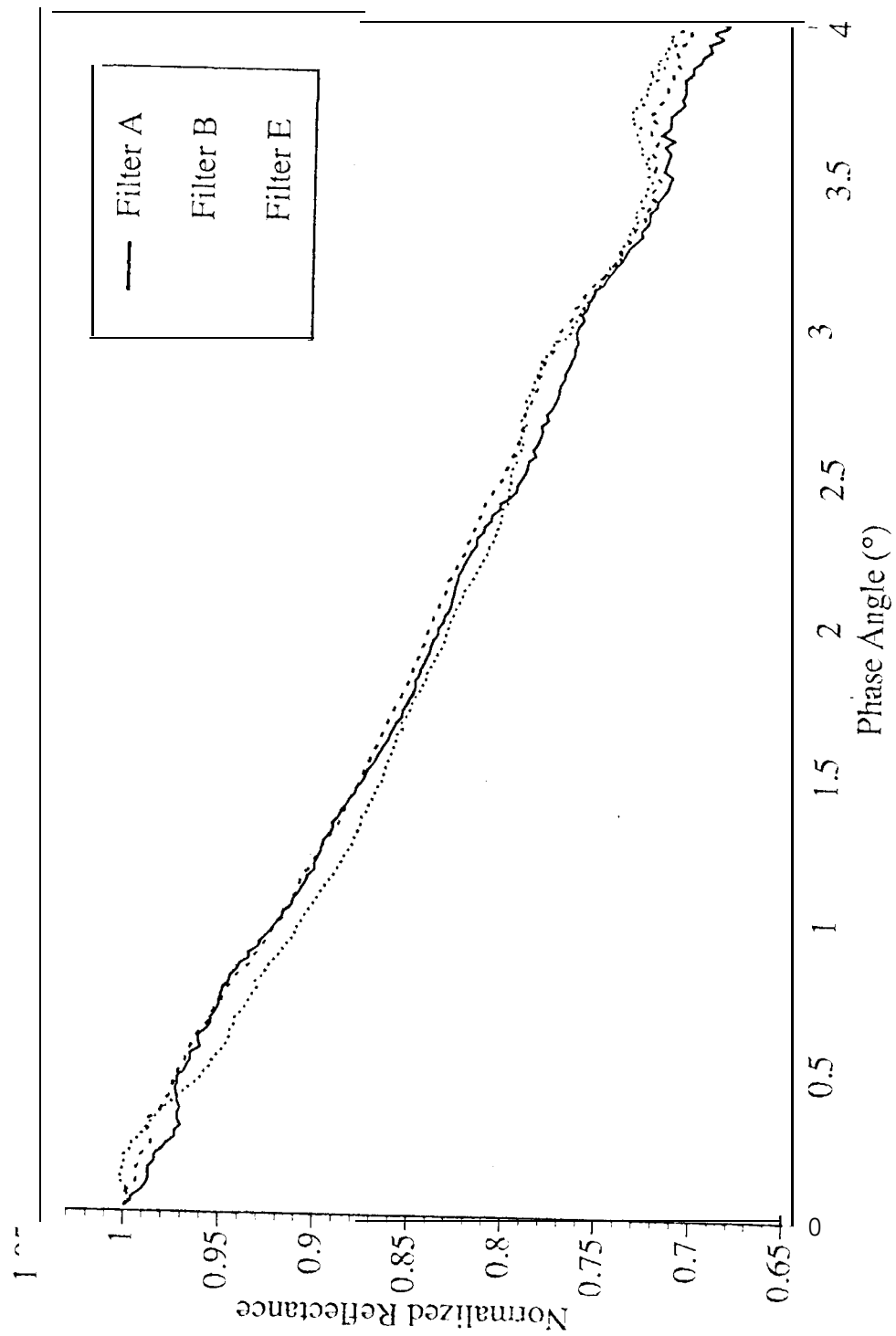


FIG. 2



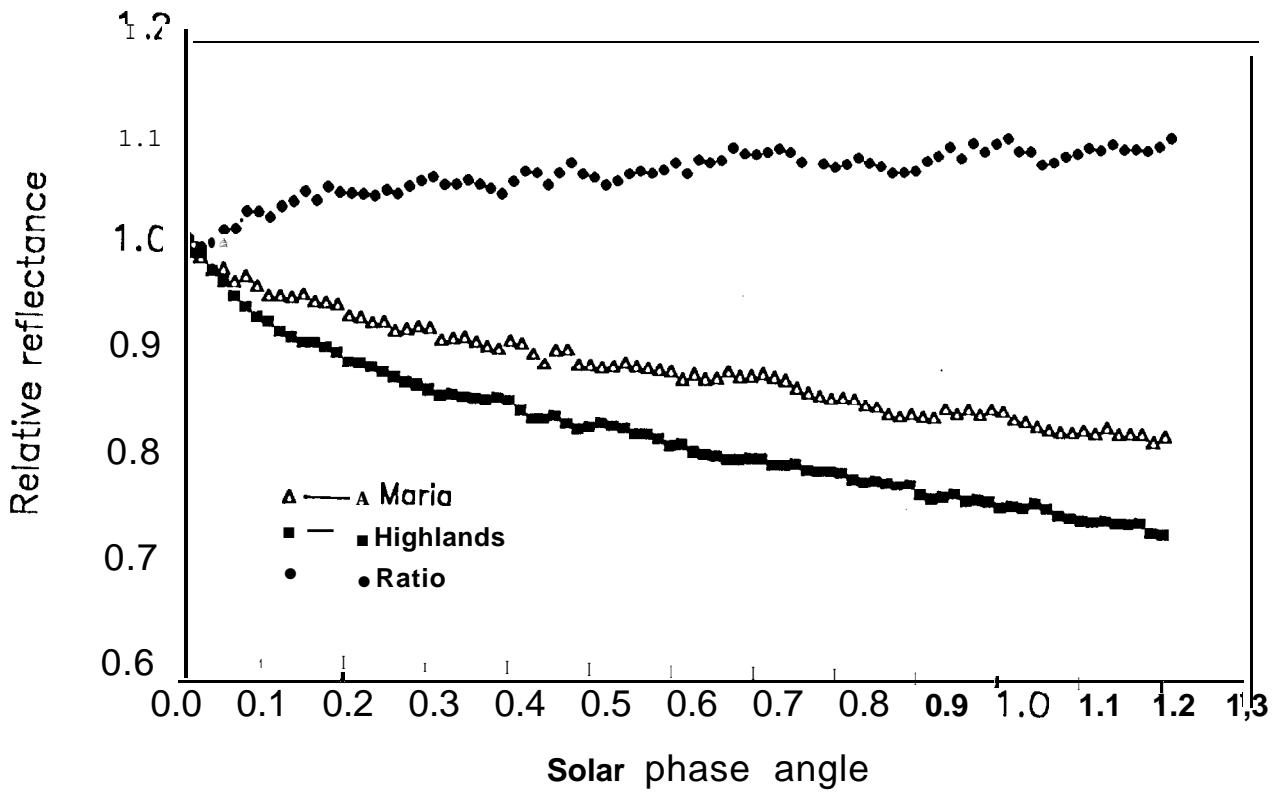


FIG. 4

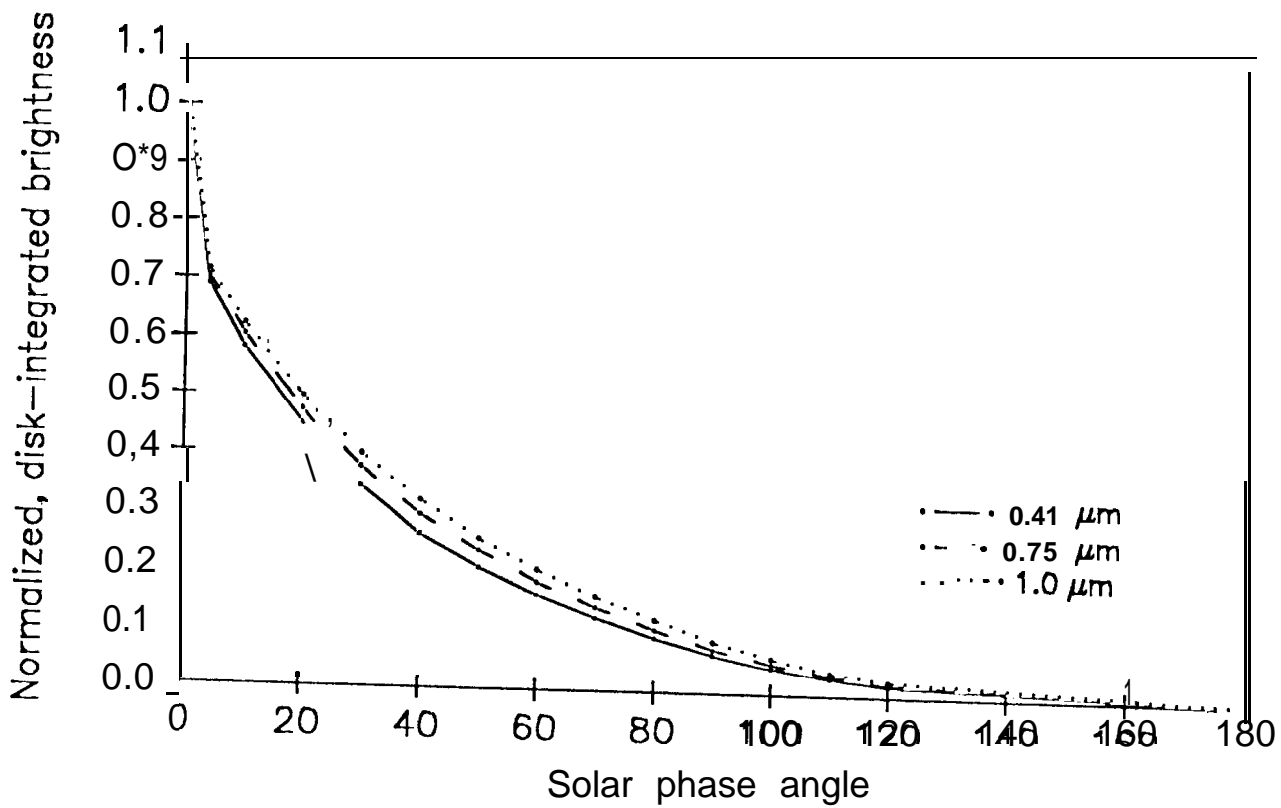


FIG. 5

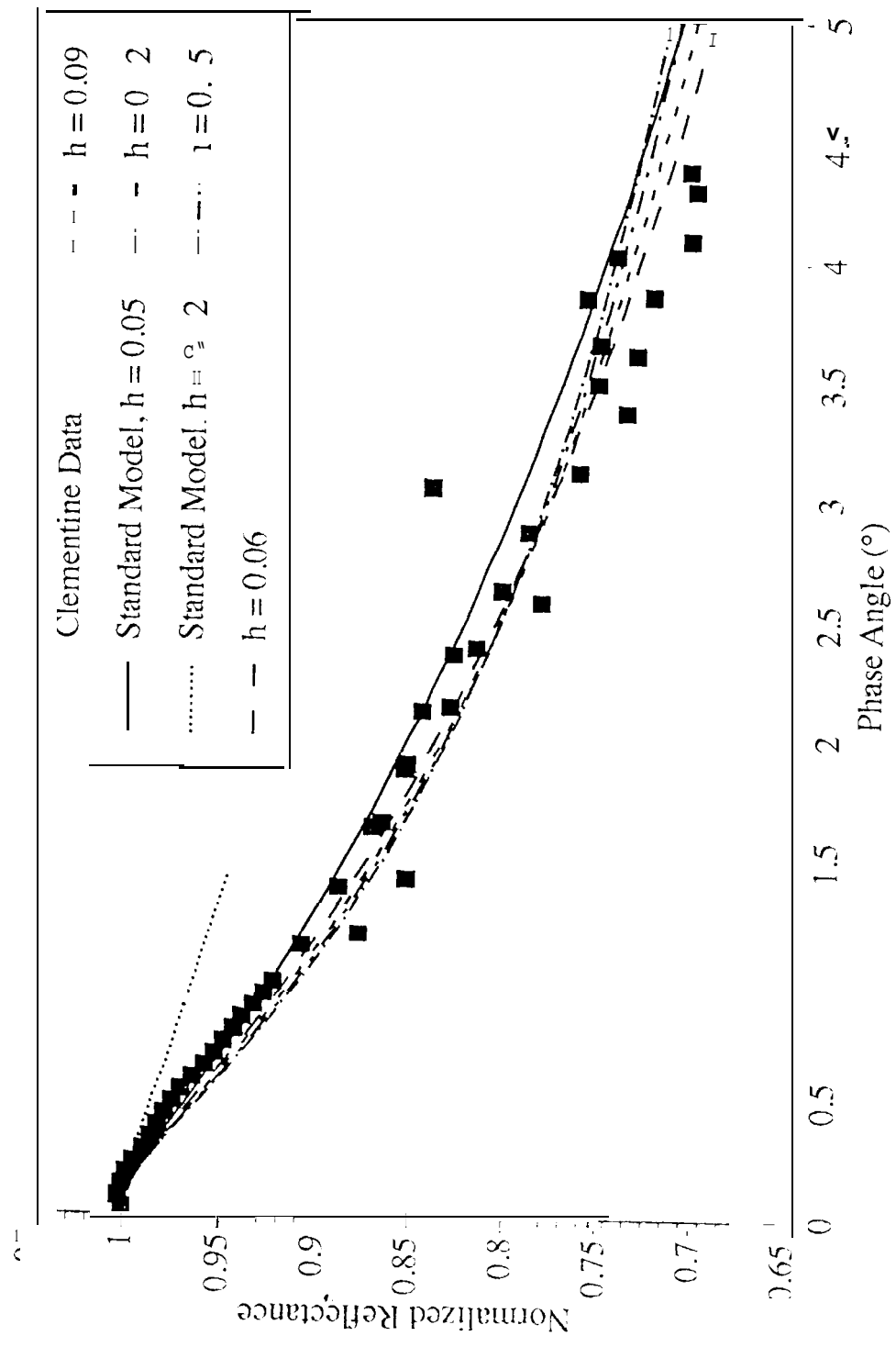


FIG. 6

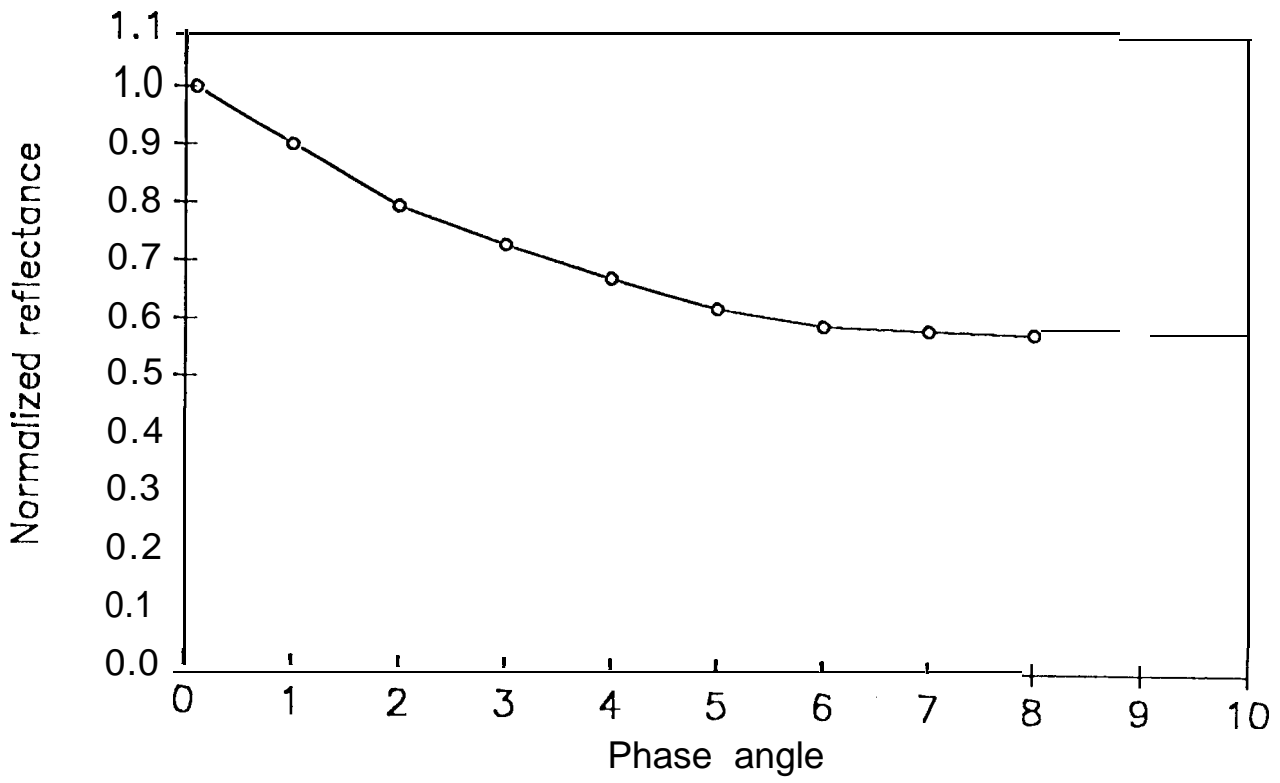


Fig. 7